

# Revisit of Cosmic Age Problem

Shuang Wang,<sup>1,2,\*</sup> Xiao-Dong Li,<sup>3,2,†</sup> and Miao Li<sup>2,4,5,‡</sup>

<sup>1</sup>*Department of Modern Physics, University of Science and Technology of China, Hefei 230026, China*

<sup>2</sup>*Institute of Theoretical Physics, Chinese Academy of Sciences, Beijing 100080, China*

<sup>3</sup>*Interdisciplinary Center for Theoretical Study, University of Science and Technology of China, Hefei 230026, China*

<sup>4</sup>*Kavli Institute for Theoretical Physics China, Chinese Academy of Sciences, Beijing 100080, China*

<sup>5</sup>*Key Laboratory of Frontiers in Theoretical Physics,  
Chinese Academy of Sciences, Beijing 100080, China*

We investigate the cosmic age problem associated with 9 extremely old globular clusters in M31 galaxy and 1 very old high- $z$  quasar APM 08279 + 5255 at  $z = 3.91$ . These 9 globular clusters have not been used to study the cosmic age problem in the previous literature. By evaluating the age of the universe in the  $\Lambda$ CDM model with the observational constraints from the SNIa, the BAO, the CMB, and the independent  $H_0$  measurements, we find that the existence of 5 globular clusters and 1 high- $z$  quasar are in tension (over  $2\sigma$  confidence level) with the current cosmological observations. So if the age estimates of these objects are correct, the cosmic age puzzle still remains in the standard cosmology. Moreover, we extend our investigations to the cases of the interacting dark energy models. It is found that although the introduction of the interaction between dark sectors can give a larger cosmic age, the interacting dark energy models still have difficulty to pass the cosmic age test.

## I. INTRODUCTION

Before the great discovery that our universe is undergoing an accelerated expansion [1, 2], the most popular cosmological model was the SCDM model (i.e., a flat universe with the present fractional matter density  $\Omega_m = 1$ ). However, the SCDM model is always plagued by a longstanding puzzle: in this model the present age of the universe is  $t_0 = \frac{2}{3H_0} \simeq 9$  Gyr ( $H_0$  denotes the Hubble constant), while astronomers have already discovered that many objects are older than 10 Gyr [3]. This so-called cosmic age problem becomes more acute if one considers the age of the universe at a high redshift. For instance, a 3.5 Gyr-old galaxy 53W091 at redshift  $z = 1.55$  and a 4 Gyr-old galaxy 53W069 at  $z = 1.43$  are more difficult to accommodate in the SCDM model [4]. Along with the discovery of accelerated expansion of our universe and the return of the cosmological constant  $\Lambda$ , the age problem has been greatly alleviated. The 7-year WMAP observations [5] tell us that in the standard cosmological model (i.e. the  $\Lambda$ CDM model) the present cosmic age is  $t_0 = 13.75 \pm 0.11$  Gyr. Besides, it is shown that the  $\Lambda$ CDM model can also easily accommodate galaxies 53W091 and 53W069 [6]. Therefore, it is widely believed that the cosmic age problem is a “smoking-gun” evidence for the standard cosmological model, and many people believe that the cosmic age puzzle does not exist in the  $\Lambda$ CDM model. However, we still want to raise the question: Is the cosmic age problem really removed by the  $\Lambda$ CDM model?

In a recent paper [7], by comparing photometric data acquired from the Beijing-Arizona-Taiwan-Connecticut (BATC) system with up-to-date theoretical synthesis models, the ages of 35 globular clusters (GCs) in M31 galaxy were estimated by Ma et al. Soon after, the ages of other 104 GCs in M31 galaxy were also obtained by the same research group [8]. From their results, we find that 9 extremely old GCs are older than the present cosmic age ( $t_0 = 13.75$  Gyr) predicted by the 7-year WMAP observations (see Table 1). To our present knowledge, these 9 GCs have not been used to study the cosmic age problem in the previous literature; so it is interesting to explore implications of these 9 old GCs for the standard cosmology. In addition, the existence of high- $z$  quasar APM 08279 + 5255 at  $z = 3.91$  [9, 10] still remains a mystery [10–14]. Using the maximum likelihood values of the 7-year WMAP observations  $\Omega_m = 0.272$  and  $h = 0.704$  ( $h$  is the reduced Hubble parameter) [5], it is seen that the  $\Lambda$ CDM model can only give a cosmic age  $t = 1.63$  Gyr at  $z = 3.91$ , while the lower limit of the quasar’s age is 1.8 Gyr [10]. In a previous paper [14], Wang and Zhang demonstrated that by simply introducing the dark energy (DE) alone we cannot remove the high- $z$  age problem, and suggested that the introduction of interaction between dark sectors may be helpful to alleviate the cosmic age problem. But in [14], when evaluating the age of the universe in the interacting DE models, the parameters describing interaction strength were chosen arbitrarily. A consistent quantitative analysis should use

---

\*Electronic address: swang@mail.ustc.edu.cn

†Electronic address: renzhe@mail.ustc.edu.cn

‡Electronic address: mli@itp.ac.cn

TABLE I: The ages of 9 extremely old Globular Clusters in M31 Galaxy. Notice that the present cosmic age predicted by the 7-year WMAP observations is  $t_0 = 13.75 \pm 0.11$  Gyr.

Object	Age(Gyr)	Reference
B024	$15.25 \pm 0.75$	Table 5 of [8]
B050	$16.00 \pm 0.30$	Table 5 of [7]
B129	$15.10 \pm 0.70$	Table 5 of [7]
B144D	$14.36 \pm 0.95$	Table 5 of [8]
B239	$14.50 \pm 2.05$	Table 5 of [7]
B260	$14.30 \pm 0.50$	Table 5 of [8]
B297D	$15.18 \pm 0.85$	Table 5 of [8]
B383	$13.99 \pm 1.05$	Table 5 of [8]
B495	$14.54 \pm 0.55$	Table 5 of [8]

the maximum likelihood method to determine the corresponding model parameters from the current cosmological observations. Then using the obtained results one can analyze the consistency with the cosmic age data. This analysis will be done in the present work.

This paper is organized as follows. In section II, we evaluate the age of the universe in the  $\Lambda$ CDM model with constraints from the Type Ia supernovae (SNIa), the Baryon Acoustic Oscillations (BAO), the Cosmic Microwave Background (CMB), and the independent  $H_0$  measurements, then use the obtained results to analyze the consistency with the age data listed above. In section III, we extend our investigation to the cases of three interacting dark energy models. We summarize in Section IV. Appendix A supplies the details of how to utilize the cosmological observations to constrain DE models. We assume today's scale factor  $a_0 = 1$ , so the redshift  $z = a^{-1} - 1$ , the subscript "0" always indicates the present value of the corresponding quantity.

## II. COSMIC AGE PROBLEM IN THE $\Lambda$ CDM MODEL

The age  $t(z)$  of a flat universe at redshift  $z$  is [11]

$$t(z) = \int_z^\infty \frac{d\tilde{z}}{(1 + \tilde{z})H(\tilde{z})}, \quad (1)$$

where  $H(z)$  is the Hubble parameter, given by the Friedman equation,

$$3M_{Pl}^2 H^2 = \rho_m + \rho_{de} + \rho_r, \quad (2)$$

$M_{Pl} \equiv 1/\sqrt{8\pi G}$  is the reduced Planck mass,  $\rho_m$ ,  $\rho_{de}$ , and  $\rho_r$  are the energy density of matter, dark energy, and radiation, respectively. The reduced Hubble parameter is  $E(z) \equiv H(z)/H_0$ . Once  $E(z)$  is given, the cosmic age  $t(z)$  at any redshift  $z$  can be evaluated. For  $\Lambda$ CDM model,

$$E(z) = \sqrt{\Omega_r(1+z)^4 + \Omega_m(1+z)^3 + 1 - \Omega_m - \Omega_r}, \quad (3)$$

where  $\Omega_r$  is the present fractional radiation density given by [5],

$$\Omega_r = \Omega_\gamma(1 + 0.2271N_{eff}), \quad \Omega_\gamma = 2.469 \times 10^{-5}h^{-2}, \quad N_{eff} = 3.04. \quad (4)$$

Note that in a flat universe the present fractional DE density is  $\Omega_{de} = 1 - \Omega_m - \Omega_r$ . Since we also consider effects of radiation component, there are two model parameters,  $\Omega_m$  and  $h$ , need to be determined.

To constrain DE models by using cosmological observations, we will employ the  $\chi^2$  statistics [15]. For a physical quantity  $\xi$  with an experimentally measured value  $\xi_{obs}$ , a standard deviation  $\sigma_\xi$ , and a theoretically predicted value  $\xi_{th}$ , the  $\chi^2$  value is given by

$$\chi_\xi^2 = \frac{(\xi_{th} - \xi_{obs})^2}{\sigma_\xi^2}. \quad (5)$$

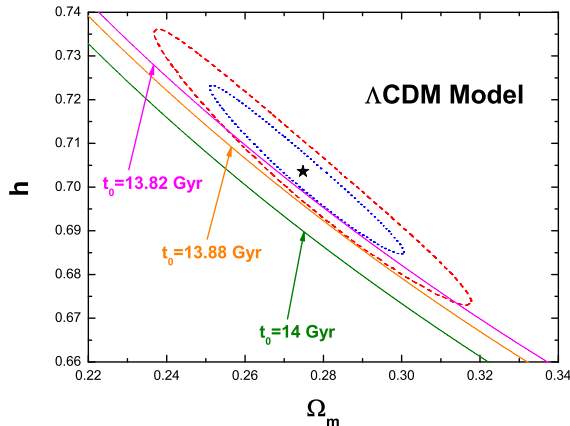


FIG. 1: Cosmic age problem at  $z = 0$  in the  $\Lambda$ CDM model. The dotted elliptical line, the dashed elliptical line, and the central star symbol denote the  $1\sigma$  confidence region, the  $2\sigma$  confidence region, and the best-fit point of the  $\Lambda$ CDM model in the  $\Omega_m$ - $h$  plane, respectively. Three solid diagonal lines, from top to bottom, represent the constraints of 13.82 Gyr, 13.88 Gyr, and 14 Gyr at  $z = 0$ , respectively. Notice that the top diagonal line tangents to the  $1\sigma$  confidence region of the  $\Lambda$ CDM model, while the middle diagonal line tangents to the  $2\sigma$  confidence region of the  $\Lambda$ CDM model. For a given diagonal line, the area below this diagonal line corresponds to a larger cosmic age. The  $\Lambda$ CDM model predicts a lower cosmic age than the  $1\sigma$  lower limits of 5 GCs' age.

The total  $\chi^2$  is the sum of all  $\chi_\xi^2$ s, i.e.,

$$\chi^2 = \sum_{\xi} \chi_\xi^2. \quad (6)$$

The model parameters yielding a minimal  $\chi^2$  is favored by observations. The observational data used in this paper include the Constitution SNIa sample [16], the BAO data from the SDSS Data Release 7 (DR7) galaxy sample [17], the CMB measurements given by the 7-year WMAP observations [5], and the independent  $H_0$  measurements from HST [18] (see Appendix A for details). With these observational data, the cosmological constraints on the  $\Lambda$ CDM model are obtained:  $\Omega_m = 0.275^{+0.026}_{-0.024}$  and  $h = 0.704^{+0.020}_{-0.019}$  at  $1\sigma$  confidence level (CL), while  $\Omega_m = 0.275^{+0.043}_{-0.038}$  and  $h = 0.704^{+0.033}_{-0.031}$  at  $2\sigma$  CL.

Now we discuss the cosmic age problem associated with those 9 extremely old GCs in M31 galaxy. The results are given in Fig.1. Our method is as follows. Firstly, since in a flat universe the age problem is mainly constrained by observational data of  $(\Omega_m, h)$ , by using the current cosmological observations (SNIa+BAO+CMB+ $H_0$ ), we plot the  $1\sigma$  and the  $2\sigma$  confidence regions of the  $\Lambda$ CDM model in the  $\Omega_m$ - $h$  plane. Secondly, since a specific cosmic age corresponds to a specific diagonal line in the  $\Omega_m$ - $h$  plane and a larger cosmic age corresponds to a lower diagonal line, by searching the diagonal line that tangents to the  $2\sigma$  confidence region of the  $\Lambda$ CDM model, we obtain the theoretical upper limit of present cosmic age (at  $2\sigma$  CL) predicted by the  $\Lambda$ CDM model. As seen in the figure, this theoretical upper limit is  $t_0 \leq 13.88$  Gyr. Notice that this upper limit is only given by the combined SNIa+BAO+CMB+ $H_0$  data, and has nothing to do with the age data of those GCs. Thirdly, we compare this theoretical upper limit of present cosmic age with the observational lower limits of those old GCs' ages listed in Table 1, and find that the  $1\sigma$  lower limits of 5 GCs' age (including B024 with a lower limit 14.50 Gyr, B050 with a lower limit 15.70 Gyr, B129 with a lower limit 14.40 Gyr, B297D with a lower limit 14.33 Gyr, and B495 with a lower limit 13.99 Gyr) are even larger than 13.88 Gyr. So the existence of these 5 GCs are in tension (over  $2\sigma$  CL) with the current cosmological observations. This means that if the age estimates of these 5 GCs [7, 8] are correct, the cosmic age puzzle still remains in the standard cosmology. It should be mentioned that during this analysis, only 9 most discrepant GCs are used to quote statistical discrepancy. One may wonder what the discrepancy is when all objects are taken into account. By treating all those 139 GCs in M31 galaxy as data points and utilizing the  $\chi^2$  statistics, this issue is also checked. We find that the  $\Lambda$ CDM model can accommodate 127 GCs, and the statistical discrepancy disappears when all objects are included.

Next we turn to the high- $z$  cosmic age problem associated with quasar APM 08279 + 5255 at  $z = 3.91$ . The age of this quasar had been estimated by studying its chemical evolution. Based on the evolution of Fe/O ratio from the X-ray observation, Ref. [9] gave a rough estimate  $t_{QSO} = (2.0 \sim 3.0)$  Gyr at  $z = 3.91$ . Soon after, by using a

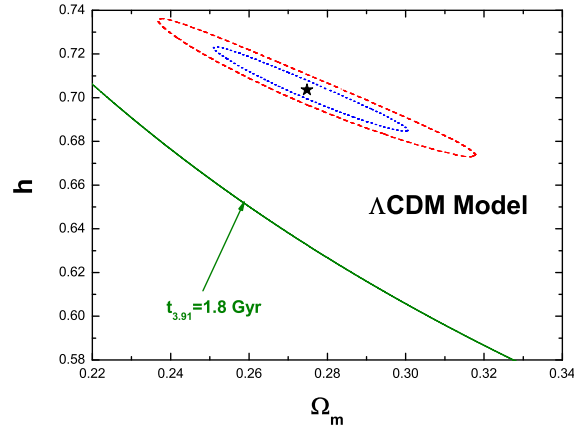


FIG. 2: High- $z$  cosmic age problem at  $z = 3.91$  in the  $\Lambda$ CDM model. The dotted elliptical line, the dashed elliptical line, and the central star symbol denote the  $1\sigma$  confidence region, the  $2\sigma$  confidence region, and the best-fit point of the  $\Lambda$ CDM model in the  $\Omega_m$ - $h$  plane, respectively. The solid diagonal line represents the lower limit of the quasar's age (i.e. 1.8 Gyr) at  $z = 3.91$ . The area below this diagonal line corresponds to a cosmic age larger than 1.8 Gyr. The  $\Lambda$ CDM model predicts a lower cosmic age than the  $1\sigma$  lower limit of the old quasar's age.

detailed chemodynamical model for the evolution of spheroid, Friaca et al. [10] obtained  $t_{QSO} = 2.1 \pm 0.3$  Gyr at the same redshift. The high- $z$  cosmic age problem at  $z = 3.91$  in the  $\Lambda$ CDM model is demonstrated in Fig.2. The method of analysis is same as that used in Fig.1. Notice that the solid diagonal line represents the  $1\sigma$  lower limit of the quasar's age (i.e. 1.8 Gyr) at  $z = 3.91$ . Our calculations show that the existence of quasar 08279 + 5255 is evidently inconsistent with the current cosmological observations, and the discrepancy is over  $7\sigma$  CL.

### III. COSMIC AGE PROBLEM IN THE INTERACTING DE MODELS

As seen in the previous section, the  $\Lambda$ CDM model has difficulty to pass the cosmic age test. One may ask how other DE models fare. In a previous paper [14], Wang and Zhang demonstrated that by simply introducing the DE alone we cannot remove the high- $z$  age problem, and suggested that the introduction of interaction between dark sectors may be helpful to alleviate the cosmic age problem. So in this work, we also investigate the cosmic age problem in the interacting DE models. As examples, three kinds of interacting DE models are considered here. In the first subsection, we introduce these 3 interacting DE models, and determine their model parameters by using cosmological observations. Then in the second subsection, we evaluate the age of the universe in these 3 models, and use the obtained results to analyze the consistency with the age data listed above.

#### A. Cosmological Constraints on Three Interacting DE Models

The universe is filled with three classes of major energy components: matter (including baryons and dark matter), dark energy, and radiation. After introducing interaction between dark sectors, the dynamical evolutions of these 3 components satisfy

$$\dot{\rho}_m + 3H\rho_m = Q \quad (7)$$

$$\dot{\rho}_{de} + 3H(\rho_{de} + p_{de}) = -Q \quad (8)$$

$$\dot{\rho}_r + 4H\rho_r = 0 \quad (9)$$

where the over dot denotes the derivative with respect to the cosmic time  $t$ ,  $Q$  denotes the phenomenological interaction term, and  $p_{de}$  is the pressure of DE given by the specific model.

We consider a simple scalar DE model with Lagrangian [19]

$$L = \frac{1}{2} \partial^\mu \phi \partial_\mu \phi - V(\phi). \quad (10)$$

Assuming the potential energy  $V(\phi)$  be dominant, the energy density and the pressure of DE are

$$\rho_{de} = -p_{de} \simeq V. \quad (11)$$

This means that the equation of state of DE  $w \equiv p_{de}/\rho_{de} = -1$ . Noting that  $a = \frac{1}{1+z}$ ,  $H = \frac{\dot{a}}{a}$ , we have

$$\frac{d}{dz} = \frac{d}{dt} \frac{dt}{da} \frac{da}{dz} = -\frac{1}{H(1+z)} \frac{d}{dt}. \quad (12)$$

Then Eqs.(7-9) can be rewritten as

$$(1+z) \frac{d\rho_m}{dz} - 3\rho_m = -Q/H \quad (13)$$

$$(1+z) \frac{d\rho_{de}}{dz} = Q/H \quad (14)$$

$$(1+z) \frac{d\rho_r}{dz} - 4\rho_r = 0 \quad (15)$$

Eq.(15) has a general solution  $\rho_r = \rho_{r0}(1+z)^4$ , while the solutions of Eqs.(13) and (14) depend on the specific form of  $Q$ .

Owing to lack of the knowledge of microscopic origin of the interaction, here we just follow [20] and consider three classes of interaction terms

$$Q_1 = 3\alpha H \rho_m \quad (16)$$

$$Q_2 = 3\alpha H \rho_{de} \quad (17)$$

$$Q_3 = 3\alpha H (\rho_m + \rho_{de}) \quad (18)$$

where  $\alpha$  is a model parameter denoting the strength of interaction. For simplicity, we will denote these 3 models by IACDM1, IACDM2, and IACDM3, respectively. Notice that all these interacting DE models have 3 model parameters,  $\Omega_m$ ,  $\alpha$ , and  $h$ .

First we discuss the IACDM1 model. Substituting  $Q_1 = 3\alpha H \rho_m$  into Eq.(13), we have

$$\rho_m = \rho_{m0}(1+z)^{3(1-\alpha)}. \quad (19)$$

Substituting Eq.(19) into Eq.(14) and using the initial condition  $\rho_{de}(z=0) = \rho_{de0}$ , we get

$$\rho_{de} = \frac{\alpha \rho_{m0}}{1-\alpha} (1+z)^{3(1-\alpha)} - \frac{\alpha \rho_{m0}}{1-\alpha} + \rho_{de0}. \quad (20)$$

Combining Eqs.(19), (20), and (2), we obtain the reduced Hubble parameter of the IACDM1 model

$$E(z) = \sqrt{\Omega_r(1+z)^4 + \frac{\Omega_m}{1-\alpha}(1+z)^{3(1-\alpha)} + (1-\Omega_r - \frac{\Omega_m}{1-\alpha})}. \quad (21)$$

Based on the  $\chi^2$  statistics method and observational data, the model parameters of the IACDM1 model are determined as  $\Omega_m = 0.279_{-0.027}^{+0.028}$ ,  $\alpha = (-1.20 \times 10^{-3})_{-3.14 \times 10^{-3}}^{+3.45 \times 10^{-3}}$ , and  $h = 0.705_{-0.019}^{+0.020}$  at  $1\sigma$  CL, while  $\Omega_m = 0.279_{-0.043}^{+0.047}$ ,  $\alpha = (-1.20 \times 10^{-3})_{-5.01 \times 10^{-3}}^{+5.78 \times 10^{-3}}$ , and  $h = 0.705_{-0.031}^{+0.033}$  at  $2\sigma$  CL.

We now turn to the IACDM2 model. Substituting  $Q_2 = 3\alpha H \rho_{de}$  into Eq.(14), we have

$$\rho_{de} = \rho_{de0}(1+z)^{3\alpha}. \quad (22)$$

Substituting Eq.(22) into Eq.(13) and using the initial condition  $\rho_m(z=0) = \rho_{m0}$ , we get

$$\rho_m = \rho_{m0}(1+z)^3 - \frac{\alpha \rho_{de0}}{1-\alpha} (1+z)^3 + \frac{\alpha \rho_{de0}}{1-\alpha} (1+z)^{3\alpha}. \quad (23)$$

Combining Eqs.(22), (23), and (2), we obtain the reduced Hubble parameter of IACDM2 model

$$E(z) = \sqrt{\Omega_r(1+z)^4 + \frac{\Omega_m - \alpha + \alpha \Omega_r}{1-\alpha} (1+z)^3 + \frac{1 - \Omega_m - \Omega_r}{1-\alpha} (1+z)^{3\alpha}}. \quad (24)$$

The model parameters of the IACDM2 model are determined as  $\Omega_m = 0.276_{-0.026}^{+0.028}$ ,  $\alpha = (-1.43 \times 10^{-3})_{-1.58 \times 10^{-2}}^{+1.34 \times 10^{-2}}$ , and  $h = 0.702_{-0.024}^{+0.026}$  at  $1\sigma$  CL, while  $\Omega_m = 0.276_{-0.042}^{+0.046}$ ,  $\alpha = (-1.43 \times 10^{-3})_{-2.75 \times 10^{-2}}^{+2.10 \times 10^{-2}}$ , and  $h = 0.702_{-0.038}^{+0.043}$  at  $2\sigma$  CL.

Next we consider the IACDM3 model. Substituting  $Q_3 = 3\alpha H(\rho_m + \rho_{de})$  into Eqs.(13) and (14), we have

$$(1+z)\frac{d\rho_m}{dz} = 3(1-\alpha)\rho_m - 3\alpha\rho_{de} \quad (25)$$

$$(1+z)\frac{d\rho_{de}}{dz} = 3\alpha(\rho_m + \rho_{de}) \quad (26)$$

Utilizing the initial conditions  $\rho_m(z=0) = \rho_{m0}$  and  $\rho_{de}(z=0) = \rho_{de0}$ , the differential equations (25) and (26) are solved as

$$\rho_m = C_1(1+z)^{k_1} + C_2(1+z)^{k_2}, \quad \rho_{de} = C_1\frac{3-3\alpha-k_1}{3\alpha}(1+z)^{k_1} + C_2\frac{3-3\alpha-k_2}{3\alpha}(1+z)^{k_2}, \quad (27)$$

where

$$k_1 = \frac{3}{2}(1 + \sqrt{1-4\alpha}), \quad k_2 = \frac{3}{2}(1 - \sqrt{1-4\alpha}), \quad (28)$$

and

$$C_1 = \frac{(3-3\alpha-k_2)\rho_{m0} - 3\alpha\rho_{de0}}{k_1 - k_2}, \quad C_2 = \frac{(3-3\alpha-k_1)\rho_{m0} - 3\alpha\rho_{de0}}{k_2 - k_1}. \quad (29)$$

From the Friedman equation, we obtain the reduced Hubble parameter of the IACDM3 model

$$E(z) = \sqrt{\Omega_r(1+z)^4 + \tilde{C}_1\frac{3-k_1}{3\alpha}(1+z)^{k_1} + \tilde{C}_2\frac{3-k_2}{3\alpha}(1+z)^{k_2}} \quad (30)$$

where

$$\tilde{C}_1 = \frac{(3-3\alpha-k_2)\Omega_m - 3\alpha(1-\Omega_m-\Omega_r)}{k_1 - k_2}, \quad \tilde{C}_2 = \frac{(3-3\alpha-k_1)\Omega_m - 3\alpha(1-\Omega_m-\Omega_r)}{k_2 - k_1}. \quad (31)$$

Parameters of the IACDM3 model are determined as  $\Omega_m = 0.279_{-0.027}^{+0.028}$ ,  $\alpha = (-8.98 \times 10^{-4})_{-2.72 \times 10^{-3}}^{+2.86 \times 10^{-3}}$ , and  $h = 0.704_{-0.019}^{+0.019}$  at  $1\sigma$  CL, while  $\Omega_m = 0.279_{-0.043}^{+0.047}$ ,  $\alpha = (-8.98 \times 10^{-4})_{-4.42 \times 10^{-3}}^{+4.70 \times 10^{-3}}$ , and  $h = 0.704_{-0.030}^{+0.032}$  at  $2\sigma$  CL.

## B. Age Problem of Three Interacting DE Models

In this subsection, we evaluate the age of the universe in these 3 interacting DE models, and analyze the consistency with the age data listed above. Since in a flat universe the age problem is mainly constrained by the observational data of  $(\Omega_m, h)$ , our results are given in the  $\Omega_m$ - $h$  plane. The method of analysis is same as that used in section II.

We plot Fig.3 to demonstrate the cosmic age problem in the IACDM1 model. The left panel of Fig.3 represents the cosmic age problem at  $z=0$ . From this panel, it is found that in the IACDM1 model, the present cosmic age  $t_0 \leq 14.02$  Gyr at  $2\sigma$  CL. Although the IACDM1 model can give an upper limit of the present cosmic age 0.14 Gyr larger than that given by the  $\Lambda$ CDM model, this cosmic age upper limit is still smaller than the  $1\sigma$  lower limits of 4 GCs' age (including B024 with a lower limit 14.50 Gyr, B050 with a lower limit 15.70 Gyr, B129 with a lower limit 14.40 Gyr, and B297D with a lower limit 14.33 Gyr). So the IACDM1 model still cannot pass the cosmic age test of these 4 GCs. We also check what the discrepancy is when all 139 GCs are taken into account. It is found that the IACDM1 model can accommodate 127 GCs, and the statistical discrepancy disappears when all objects are included. Besides, the right panel of Fig.3 represents the high- $z$  cosmic age problem at  $z=3.91$ . Our calculations show that the existence of high- $z$  quasar APM 08279 + 5255 cannot be accommodated in the IACDM1 model, and the discrepancy is at  $5\sigma$  CL.

The situation of the IACDM2 model is demonstrated in the Fig.4. The left panel of Fig.4 represents the cosmic age problem at  $z=0$ . From this panel, it is found that in the IACDM2 model, the present cosmic age  $t_0 \leq 14.03$  Gyr at  $2\sigma$  CL. Although the IACDM2 model can give an upper limit of the present cosmic age 0.15 Gyr larger than that given by the  $\Lambda$ CDM model, this cosmic age upper limit is still smaller than the  $1\sigma$  lower limits of 4 GCs' age (including B024, B050, B129, and B297D). We also check what the discrepancy is when all 139 GCs are taken into

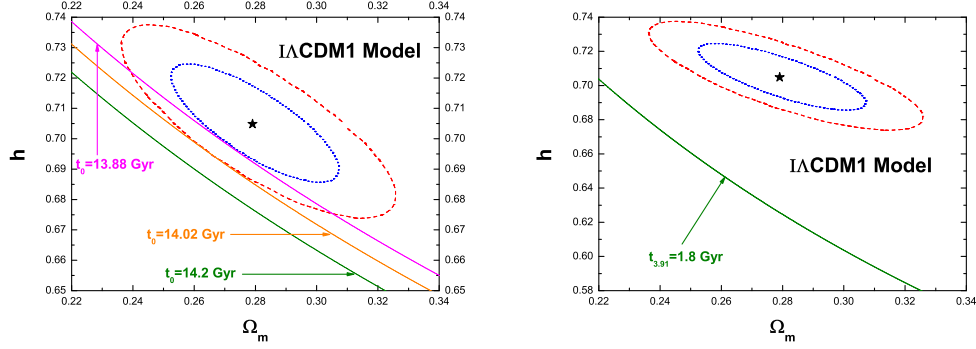


FIG. 3: Cosmic age problem in IACDM1 model. The dotted elliptical line, the dashed elliptical line, and the central star symbol denote the  $1\sigma$  confidence region, the  $2\sigma$  confidence region, and the best-fit point of the IACDM1 model in the  $\Omega_m$ - $h$  plane, respectively. In the left panel, three solid diagonal lines, from top to bottom, represent the constraints of 13.88 Gyr, 14.02 Gyr, and 14.2 Gyr at  $z = 0$ , respectively. When plotting these diagonal lines denoting cosmic age constraints, the best-fit value of interaction strength of IACDM1 model  $\alpha = -1.20 \times 10^{-3}$  is adopted. Notice that the top diagonal line tangents to the  $1\sigma$  confidence region of the IACDM1 model, while the middle diagonal line tangents to the  $2\sigma$  confidence region of the IACDM1 model. In the right panel, the solid diagonal line represents the lower limit of the quasar's age at  $z = 3.91$ . The area below this diagonal line corresponds to a cosmic age larger than 1.8 Gyr. The IACDM1 model predicts a lower cosmic age than the  $1\sigma$  lower limits of 4 GCs' age, and also predicts a lower cosmic age than the  $1\sigma$  lower limit of the old quasar's age.

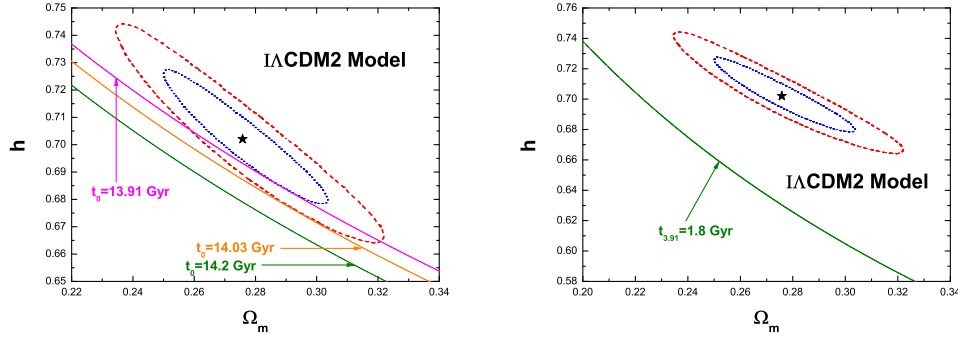


FIG. 4: Cosmic age problem in the IACDM2 model. The dotted elliptical line, the dashed elliptical line, and the central star symbol denote the  $1\sigma$  confidence region, the  $2\sigma$  confidence region, and the best-fit point of the IACDM2 model in the  $\Omega_m$ - $h$  plane, respectively. In the left panel, three solid diagonal lines, from top to bottom, represent the constraints of 13.91 Gyr, 14.03 Gyr, and 14.2 Gyr at  $z = 0$ , respectively. When plotting these diagonal lines denoting cosmic age constraints, the best-fit value of interaction strength of the IACDM2 model  $\alpha = -1.43 \times 10^{-3}$  is adopted. Notice that the top diagonal line tangents to the  $1\sigma$  confidence region of the IACDM2 model, while the middle diagonal line tangents to the  $2\sigma$  confidence region of the IACDM2 model. In the right panel, the solid diagonal line represents the lower limit of the quasar's age at  $z = 3.91$ . The area below this diagonal line corresponds to a cosmic age larger than 1.8 Gyr. The IACDM2 model predicts a lower cosmic age than the  $1\sigma$  lower limits of 4 GCs' age, and also predicts a lower cosmic age than the  $1\sigma$  lower limit of the old quasar's age.

account. It is found that the IACDM2 model can accommodate 127 GCs, and the statistical discrepancy disappears when all objects are included. Besides, the right panel of Fig.4 represents the high- $z$  cosmic age problem at  $z = 3.91$ . Our calculations show that the IACDM2 model cannot pass the cosmic age test of the quasar APM 08279 + 5255, and the discrepancy is at  $6\sigma$  CL.

The situation of the IACDM3 model is shown in the Fig.5. The left panel of Fig.5 represents the cosmic age problem at  $z = 0$ . From this panel, it is found that in the IACDM3 model, the present cosmic age  $t_0 \leq 13.94$  Gyr at  $2\sigma$  CL. Although the IACDM3 model can give an upper limit of the present cosmic age larger than that given by the  $\Lambda$ CDM model, this cosmic age upper limit is still smaller than the  $1\sigma$  lower limits of 5 GCs' age. We also check what the discrepancy is when all 139 GCs are taken into account. It is found that the IACDM3 model can accommodate 127 GCs, and the statistical discrepancy disappears when all objects are included. Besides, the right panel of Fig.5

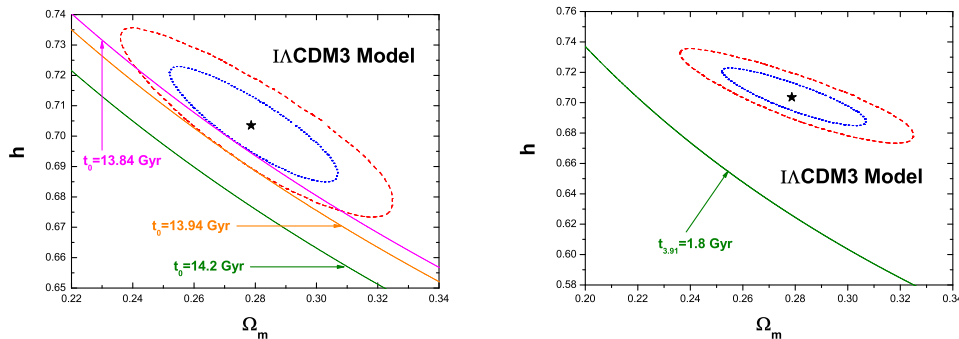


FIG. 5: Cosmic age problem in the IACDM3 model. The dotted elliptical line, the dashed elliptical line, and the central star symbol denote the  $1\sigma$  confidence region, the  $2\sigma$  confidence region, and the best-fit point of the IACDM3 model in the  $\Omega_m$ - $h$  plane, respectively. In the left panel, three solid diagonal lines, from top to bottom, represent the constraints of 13.84 Gyr, 13.94 Gyr, and 14.2 Gyr at  $z = 0$ , respectively. When plotting those diagonal lines denoting cosmic age constraints, the best-fit value of interaction strength of the IACDM3 model  $\alpha = -8.98 \times 10^{-4}$  is adopted. Notice that the top diagonal line tangents to the  $1\sigma$  confidence region of the IACDM3 model, while the middle diagonal line tangents to the  $2\sigma$  confidence region of the IACDM3 model. In the right panel, the solid diagonal line represents the lower limit of the quasar's age at  $z = 3.91$ . The area below this diagonal line corresponds to a cosmic age larger than 1.8 Gyr. The IACDM3 model predicts a lower cosmic age than the  $1\sigma$  lower limits of 5 GCs' age, and also predicts a lower cosmic age than the  $1\sigma$  lower limit of the old quasar's age.

represents the high- $z$  cosmic age problem at  $z = 3.91$ . Our calculations show that the existence of high- $z$  quasar APM 08279 + 5255 cannot be accommodated in the IACDM3 model, and the discrepancy is at  $6\sigma$  CL.

Therefore, although the introduction of the interaction between dark sectors can give a larger cosmic age, the interacting dark energy models still have difficulty to pass the cosmic age test. This conclusion is different from that of [14].

#### IV. SUMMARY

The cosmic age problem is a longstanding issue, and provides an important tool for constraining the expanding history of the universe [21]. In this work, we investigate the cosmic age problem associated with 9 extremely old globular clusters in M31 galaxy and 1 very old high- $z$  quasar APM 08279 + 5255 at  $z = 3.91$ . It should be pointed out that these 9 GCs have not been used to study the cosmic age problem in the previous literature. By evaluating the age of the universe in the  $\Lambda$ CDM model with the constraints from the SNIa, the BAO, the CMB, and the independent  $H_0$  measurements, we find that the existence of 5 globular clusters and 1 high- $z$  quasar are in tension (over  $2\sigma$  confidence level) with the current cosmological observations. Therefore, if the age estimates of these objects are correct, the cosmic age puzzle still remains in the standard cosmology. Moreover, we extend our investigations to the cases of the interacting dark energy models. By studying the cosmic age problem in the three classes of interacting models, it is found that although the introduction of the interaction between dark sectors can give a larger cosmic age, the interacting DE models still have difficulty to pass the cosmic age test. This conclusion is different from that of [14]. In a latest paper [22], Cui and Zhang argue that the high- $z$  cosmic age problem can be greatly alleviated when the interaction and spatial curvature are both introduced in the holographic dark energy model [23, 24]. Therefore, the cosmic age problem still needs to be further investigated in the future work.

#### Acknowledgements

We are grateful to the referee for helpful suggestions. We would like to thank Jun Ma and Deepak Jain, for helpful discussions. This work was supported by the NSFC grant No.10535060/A050207, a NSFC group grant No.10821504 and Ministry of Science and Technology 973 program under grant No.2007CB815401. Shuang Wang was also supported by a graduate fund of USTC.



## Appendix A: Utilizing Various Cosmological Observations to constrain DE Models

First we start with the SNIa observations. We use the Constitution sample including 397 data that are given in terms of the distance modulus  $\mu_{obs}(z_i)$  [16]. The theoretical distance modulus is defined as

$$\mu_{th}(z_i) \equiv 5 \log_{10} D_L(z_i) + \mu_0, \quad (32)$$

where  $\mu_0 \equiv 42.38 - 5 \log_{10} h$  with  $h$  the Hubble constant  $H_0$  in units of 100 km/s/Mpc, and in a flat universe the Hubble-free luminosity distance  $D_L \equiv H_0 d_L$  ( $d_L$  denotes the physical luminosity distance) is

$$D_L(z) = (1+z) \int_0^z \frac{dz'}{E(z'; \theta)}, \quad (33)$$

where  $\theta$  denotes the model parameters. The  $\chi^2$  for the SNIa data is

$$\chi_{SN}^2(\theta) = \sum_{i=1}^{397} \frac{[\mu_{obs}(z_i) - \mu_{th}(z_i; \theta)]^2}{\sigma_i^2}, \quad (34)$$

where  $\mu_{obs}(z_i)$  and  $\sigma_i$  are the observed value and the corresponding  $1\sigma$  error of distance modulus for each supernova, respectively. Following Ref.[25], the minimization with respect to  $\mu_0$  can be made trivially by expanding the  $\chi^2$  of Eq. (34) with respect to  $\mu_0$  as

$$\chi_{SN}^2(\theta) = A(\theta) - 2\mu_0 B(\theta) + \mu_0^2 C, \quad (35)$$

where

$$A(\theta) = \sum_i \frac{[\mu_{obs}(z_i) - \mu_{th}(z_i; \mu_0 = 0, \theta)]^2}{\sigma_i^2}, \quad (36)$$

$$B(\theta) = \sum_i \frac{\mu_{obs}(z_i) - \mu_{th}(z_i; \mu_0 = 0, \theta)}{\sigma_i^2}, \quad (37)$$

$$C = \sum_i \frac{1}{\sigma_i^2}. \quad (38)$$

Evidently, Eq.(34) has a minimum for  $\mu_0 = B/C$  at

$$\tilde{\chi}_{SN}^2(\theta) = A(\theta) - \frac{B(\theta)^2}{C}. \quad (39)$$

Since  $\chi_{SN,min}^2 = \tilde{\chi}_{SN,min}^2$ , instead minimizing  $\chi_{SN}^2$  we minimize  $\tilde{\chi}_{SN}^2$  which is independent of the nuisance parameter  $\mu_0$ .

Next we turn to the BAO observations. The spherical average gives us the following effective distance measure [26]

$$D_V(z) \equiv \left[ (1+z)^2 D_A^2(z) \frac{z}{H(z)} \right]^{1/3}, \quad (40)$$

where  $D_A(z)$  is the proper angular diameter distance

$$D_A(z) = \frac{1}{1+z} \int_0^z \frac{dz'}{E(z')} \quad (41)$$

The BAO data from the spectroscopic SDSS DR7 galaxy sample [17] give  $D_V(z = 0.35)/D_V(z = 0.2) = 1.736 \pm 0.065$ . Thus, the  $\chi^2$  for the BAO data is,

$$\chi_{BAO}^2 = \left( \frac{D_V(z = 0.35)/D_V(z = 0.2) - 1.736}{0.065} \right)^2 \quad (42)$$

Next consider the CMB observations. Here we employ the “WMAP distance priors” given by the 7-year WMAP observations [5]. This includes the “acoustic scale”  $l_A$ , the “shift parameter”  $R$ , and the redshift of the decoupling epoch of photons  $z_*$ . The acoustic scale  $l_A$  describes the distance ratio  $D_A(z_*)/r_s(z_*)$ , defined as

$$l_A \equiv (1 + z_*) \frac{\pi D_A(z_*)}{r_s(z_*)}, \quad (43)$$

where a factor of  $(1 + z_*)$  arises because  $D_A(z_*)$  is the proper angular diameter distance, whereas  $r_s(z_*)$  is the comoving sound horizon at  $z_*$ . The fitting formula of  $r_s(z)$  is given by

$$r_s(z) = \frac{1}{\sqrt{3}} \int_0^{1/(1+z)} \frac{da}{a^2 H(a) \sqrt{1 + (3\Omega_b/4\Omega_\gamma)a}}, \quad (44)$$

where  $\Omega_b$  and  $\Omega_\gamma$  are the present-day baryon and photon density parameters, respectively. In this paper, we adopt the best-fit values,  $\Omega_b = 0.022765h^{-2}$  and  $\Omega_\gamma = 2.469 \times 10^{-5}h^{-2}$  (for  $T_{cmb} = 2.725$  K), given by the 7-year WMAP observations [5]. The fitting function of  $z_*$  is proposed by Hu and Sugiyama [27]:

$$z_* = 1048[1 + 0.00124(\Omega_b h^2)^{-0.738}][1 + g_1(\Omega_m h^2)^{g_2}], \quad (45)$$

where

$$g_1 = \frac{0.0783(\Omega_b h^2)^{-0.238}}{1 + 39.5(\Omega_b h^2)^{0.763}}, \quad g_2 = \frac{0.560}{1 + 21.1(\Omega_b h^2)^{1.81}}. \quad (46)$$

The shift parameter  $R$  is responsible for the distance ratio  $D_A(z_*)/H^{-1}(z_*)$ , given by [28]

$$R(z_*) \equiv \sqrt{\Omega_m H_0^2 (1 + z_*)} D_A(z_*). \quad (47)$$

Following Ref.[5], we use the prescription for using the WMAP distance priors. Thus, the  $\chi^2$  for the CMB data is

$$\chi_{CMB}^2 = (x_i^{th} - x_i^{obs})(C^{-1})_{ij}(x_j^{th} - x_j^{obs}), \quad (48)$$

where  $x_i = (l_A, R, z_*)$  is a vector, and  $(C^{-1})_{ij}$  is the inverse covariance matrix. The 7-year WMAP observations [5] give the maximum likelihood values:  $l_A(z_*) = 302.09$ ,  $R(z_*) = 1.725$ , and  $z_* = 1091.3$ . The inverse covariance matrix is also given in Ref. [5]

$$(C^{-1}) = \begin{pmatrix} 2.305 & 29.698 & -1.333 \\ 29.698 & 6825.27 & -113.180 \\ -1.333 & -113.180 & 3.414 \end{pmatrix}. \quad (49)$$

At last, we also use the prior on the present-day Hubble constant  $H_0 = 74.2 \pm 3.6$  km/s/Mpc [18]. In Ref.[18], the authors obtain this measured value of  $H_0$  from the magnitude-redshift relation of 240 low- $z$  type Ia supernovae at  $z < 0.1$ . It is remarkable that this Gaussian prior on  $H_0$  has also been used in the analysis of the WMAP 7-year observational data [5]. The  $\chi^2$  function for the Hubble constant is

$$\chi_h^2 = \left( \frac{h - 0.742}{0.036} \right)^2. \quad (50)$$

- 
- [1] A.G. Riess et al., *Astron. J* **116**, 1009 (1998).
  - [2] S. Perlmutter et al., *Astrophys. J* **517**, 565 (1999).
  - [3] B. Chaboyer, *Phys. Rept.* **307**, 23 (1998); L.M. Krauss and B. Chaboyer, *Science* **299**, 65 (2003).
  - [4] J. Dunlop et al., *Nature* **381**, 581 (1996); H. Spinrad et al., *ApJ*. **484**, 581 (1997).
  - [5] E. Komatsu et al., arXiv:1001.4538.
  - [6] J.S. Alcaniz and J.A.S. Lima *Astrophys. J* **521**, L87 (1999); J.A.S. Lima and J.S. Alcaniz, *Mon. Not. R. Astron. Soc.* **317**, 893 (2000).
  - [7] J. Ma et al., *Astron. J* **137**, 4884 (2009).

- [8] S. Wang et al., *Astron. J.* **139**, 1438 (2010).
- [9] G. Hasinger, N. Scharrel and S. Komossa, *ApJ* **573**, L77 (2002); S. Komossa and G. Hasinger, Proceedings of the Workshop XEUS Studying the Evolution of the Universe, edited by G. Hasinger et al. (to be published).
- [10] A.C.S. Friacas, J.S. Alcaniz, and J.A.S. Lima, *Mon. Not. R. Astron. Soc.* **362**, 1295 (2005).
- [11] J.S. Alcaniz, D. Jain and A. Dev, *Phys. Rev. D* **67**, 043514 (2003); D. Jain and A. Dev, *Phys. Lett. B* **633**, 436 (2006).
- [12] N. Pires, Z.H. Zhu and J.S. Alcaniz, *Phys. Rev. D* **73**, 123530 (2006); S. Rahvar and M.S. Movahed, *Phys. Rev. D* **75**, 023512 (2007); H. Wei and S.N. Zhang, *Phys. Rev. D* **76**, 063003 (2007).
- [13] B. Wang et al., *Nucl. Phys. B* **778**, 69 (2007); B. Wang et al., *Phys. Lett. B* **662**, 375 (2008).
- [14] S. Wang and Y. Zhang, *Phys. Lett. B* **669**, 201 (2008).
- [15] M. Li, X.D. Li, S. Wang and X. Zhang, *JCAP* **0906**, 036 (2009); Q.G. Huang, M. Li, X.D. Li and S. Wang, *Phys. Rev. D* **80**, 083515 (2009); M. Li, X.D. Li and S. Wang, arXiv:0910.0717.
- [16] M. Hicken et al., *ApJ* **700**, 1097 (2009).
- [17] W.J. Percival et al., *Mon. Not. R. Astron. Soc.* **401**, 2148 (2010).
- [18] A.G. Riess et al., *ApJ* **699**, 539 (2009).
- [19] B. Ratra and P.J.E. Peebles, *Phys. Rev. D* **37**, 3406 (1988); P.J.E. Peebles and B. Ratra, *ApJ* **325**, L17 (1988); R.R. Caldwell, R. Dave and P.J. Steinhardt, *Phys. Rev. Lett.* **80**, 1582 (1998); I. Zlatev, L. Wang and P.J. Steinhardt, *Phys. Rev. Lett.* **82**, 896 (1999).
- [20] M. Li et al., *JCAP* **12**, 014 (2009).
- [21] M.X. Lan, M. Li, X.D. Li and S. Wang, *Phys. Rev. D* **82**, 023516 (2010).
- [22] J.L. Cui and X. Zhang, *Phys. Lett. B* **690**, 233 (2010).
- [23] M. Li, *Phys. Lett. B* **603**, 1 (2004); Q.G. Huang and M. Li, *JCAP* **08**, 013 (2004); Q.G. Huang and M. Li, *JCAP* **03**, 001 (2005); M. Li, C.S. Lin and Y. Wang, *JCAP* **05**, 023 (2008); M. Li, X.D. Li, C.S. Lin and Y. Wang, *Commun. Theor. Phys.* **51**, 181 (2009); X. Zhang, *Phys. Lett. B* **683**, 81 (2010).
- [24] M. Li, R.X. Miao, and Y. Pang, *Phys. Lett. B* **689**, 55 (2010); M. Li, R.X. Miao, and Y. Pang, *Opt. Express* **18**, 9026 (2010).
- [25] S. Nesseris and L. Perivolaropoulos, *Phys. Rev. D* **72**, 123519 (2005).
- [26] D.J. Eisenstein et al., *ApJ* **633**, 560 (2005).
- [27] W. Hu and N. Sugiyama, *ApJ* **471**, 542 (1996).
- [28] J.R. Bond, G. Efstathiou and M. Tegmark, *Mon. Not. R. Astron. Soc.* **291**, L33 (1997).